

The $1/N$ expansion of colored tensor models

Razvan Gurau*

*Perimeter Institute for Theoretical Physics
31 Caroline St, Waterloo, Ontario N2L 2Y5, Canada*

In this paper we perform the $1/N$ expansion of the colored three dimensional Boulatov tensor model. As in matrix models, we obtain a systematic topological expansion, with increasingly complicated topologies suppressed by higher and higher powers of N . We compute the first orders of the expansion and prove that only graphs corresponding to three spheres S^3 contribute to the leading order in the large N limit.

I. INTRODUCTION

Random tensor models and Group Field Theories (GFT) [1, 2] generalize random matrix models [3–6] to higher dimensions. The Feynman graphs of GFT are built from vertices dual to n simplices, and propagators encoding the gluing of n simplices along boundary $(n-1)$ simplices. Parallel to ribbon graphs of matrix models (dual to discretized surfaces), GFT graphs are dual to discretized n dimensional topological spaces. For the simplest GFT models [7] the Feynman amplitude of a graph, reproduces the partition function of discretized BF theory [8, 9]¹.

In contrast with random matrix models, the usual GFT models suffer from two major problems. First the Feynman graphs of GFTs are dual not only to manifolds and pseudo manifolds but also to more singular spaces [14]. Second, and even more problematic, no equivalent of the $1/N$ expansion or of the notion of planarity [15] crucial in matrix models had yet been found in GFTs. This is one of the most important challenges GFTs and tensor models face today [16]. The recently introduced “colored GFTs” [17, 18] (CGFT) solve the first problem [14] and generate only pseudo manifolds. In this paper we prove that they also solve the second problem, namely CGFTs admit a $1/N$ topological expansion. We present in this paper the systematic expansion at all orders of CGFT and explicitly compute the first terms. We prove that at leading order in $1/N$ only graphs dual to the three sphere S^3 contribute. To establish this result we will rely on one hand on results and methods introduced in [19–23] concerning amplitudes of CGFT graphs and on the other on results in combinatorial topology and manifold crystallization theory [24, 25]. Almost none of the concepts and techniques we use can be applied to non colored GFT models.

This paper is organized as follows. In Section II we recall the colored three dimensional Boulatov tensor model. Sections III and IV introduce the techniques required to perform in section V the $1/N$ expansion of the model.

II. THE COLORED BOULATOV MODEL

Let G be some compact multiplicative Lie group, and denote h its elements, e its unit, and $\int dh$ the integral with respect to the Haar measure. Let $\bar{\psi}^i, \psi^i, i = 0, 1, 2, 3$ be four couples of complex scalar (or Grassmann) fields over three copies of G , $\psi^i : G \times G \times G \rightarrow \mathbb{C}$. We denote $\delta^N(h)$ the delta function over G with some cutoff such that $\delta^N(e)$ is finite, but diverges (polynomially) when N goes to infinity. For $G = SU(2)$ (denoting $\chi^j(h)$ the character of h in the representation j) respectively $G = U(1)$ we can chose

$$\delta^N(h) \Big|_{G=SU(2)} = \sum_{j=0}^N (2j+1) \chi^j(h) \quad \delta^N(\varphi) \Big|_{G=U(1)} = \sum_{p=-N}^N e^{ip\varphi} . \quad (1)$$

The partition function of the colored Boulatov model [17] over G is the path integral

$$Z(\lambda, \bar{\lambda}) = e^{-F(\lambda, \bar{\lambda})} = \int \prod_{i=0}^4 d\mu_P(\bar{\psi}^i, \psi^i) e^{-S^{int}(\bar{\psi}^i, \psi^i)} , \quad (2)$$

with normalized Gaussian measure of covariance P

$$P_{h_0 h_1 h_2; h'_0 h'_1 h'_2} = \int d\mu_P(\bar{\psi}^i, \psi^i) \bar{\psi}_{h_0 h_1 h_2}^i \psi_{h'_0 h'_1 h'_2}^i = \int dh \delta^N(h_0 h(h'_0)^{-1}) \delta^N(h_1 h(h'_1)^{-1}) \delta^N(h_2 h(h'_2)^{-1}) , \quad (3)$$

* rgurau@perimeterinstitute.ca

¹ More involved GFT models [10–13] have been proposed in an attempt to implement the Plebanski constraints and reproduce the gravity partition function.

and interaction (denoting $\psi(h, p, q) = \psi_{hpq}$)

$$\begin{aligned} \mathcal{S}^{int} &= \frac{\lambda}{\sqrt{\delta^N(e)}} \int_{G^6} \psi_{h_{03}h_{02}h_{01}}^0 \psi_{h_{10}h_{13}h_{12}}^1 \psi_{h_{21}h_{20}h_{23}}^2 \psi_{h_{32}h_{31}h_{30}}^3 \\ &+ \frac{\bar{\lambda}}{\sqrt{\delta^N(e)}} \int_{G^6} \bar{\psi}_{h_{03}h_{02}h_{01}}^0 \bar{\psi}_{h_{10}h_{13}h_{12}}^1 \bar{\psi}_{h_{21}h_{20}h_{23}}^2 \bar{\psi}_{h_{32}h_{31}h_{30}}^3, \end{aligned} \quad (4)$$

where $h_{ij} = h_{ji}$. We call ‘‘black’’ the vertex involving the ψ 's and ‘‘white’’ the one involving the $\bar{\psi}$'s.

The half lines of the CGFT vertex (represented in figure 1) have a color i . The group elements h_{ij} in eq. (4) are associated to the ‘‘strands’’ (represented as solid lines) common to the half lines i and j . The vertex is dual to a tetrahedron and its half lines represent the triangles bounding the tetrahedron. The strand ij , common to the half lines i and j , represents the edge of the tetrahedron common to the triangles i and j . The CGFT lines (figure

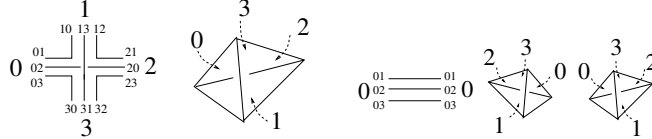


FIG. 1. Colored GFT vertex and line.

1) always connect two vertices of opposite orientation (i.e. a black and a white vertex). They have three *parallel* strands associated to the three arguments of the fields. A line represents the gluing of two tetrahedra (of opposite orientations) along triangles of the same color.

The strand structure of the vertex and propagator is fixed. One can represent a CGFT graph either as a stranded graph (using the vertex and propagator in figure 1) or as a ‘‘colored graph’’ with (colored) solid lines, and two classes of oriented vertices. Some examples of CGFT graphs are given in figure 2. We denote them from left to right \mathcal{G}_1 , \mathcal{G}_2 , $\mathcal{G}_{3;a}$, $\mathcal{G}_{3;b}$, $\mathcal{G}_{3;c}$ and $\mathcal{G}_{3;d}$.

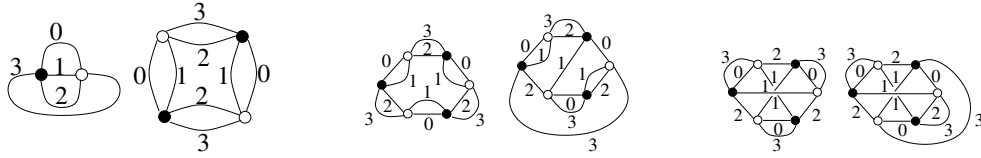


FIG. 2. Examples of Colored GFT graphs.

The lines of a vacuum CGFT graph \mathcal{G} are oriented (say from the black to the white vertex). The closed strands of \mathcal{G} form ‘‘faces’’ and are labeled by couples of colors. A vacuum CGFT graph must have the same number of black and white vertices. In this paper we will only deal with connected graphs. We denote $\mathcal{N}_{\mathcal{G}}$, $\mathcal{L}_{\mathcal{G}}$, $\mathcal{F}_{\mathcal{G}}$ the sets of vertices, lines and faces of \mathcal{G} . Also, we denote $\mathcal{L}_{\mathcal{G}}^i$ the set of lines of color i and $\mathcal{F}_{\mathcal{G}}^{ij}$ the set of faces of colors ij of \mathcal{G} . The Feynman amplitude of \mathcal{G} is

$$A^{\mathcal{G}} = \frac{(\lambda\bar{\lambda})^{\frac{\mathcal{N}_{\mathcal{G}}}{2}}}{[\delta^N(e)]^{\frac{|\mathcal{N}_{\mathcal{G}}|}{2}}} \int \prod_{\ell \in \mathcal{L}_{\mathcal{G}}} dh_{\ell} \prod_{f \in \mathcal{F}_{\mathcal{G}}} \delta_f^N \left(\prod_{\ell \in f} h_{\ell}^{\sigma^{\ell|f}} \right), \quad (5)$$

where the notation $\ell \in f$ (which we sometimes omit) signifies that the line ℓ belongs to the face f and $\sigma^{\ell|f} = 1$ (resp. -1) if the orientations of ℓ and f coincide (resp. are opposite). The δ^N functions are invariant under cyclic permutations and conjugation of their arguments hence the amplitude of a graph does not depend on the orientation of the faces or on their starting point.

The first ingredient in our $1/N$ expansion is the scaling of the coupling in eq. (4). In [21] it is proved that $A^{\mathcal{G}}$ obeys

$$A^{\mathcal{G}} \leq \frac{(\lambda\bar{\lambda})^{\frac{|\mathcal{N}_{\mathcal{G}}|}{2}}}{[\delta^N(e)]^{\frac{|\mathcal{N}_{\mathcal{G}}|}{2}}} [\delta^N(e)]^{\frac{|\mathcal{N}_{\mathcal{G}}|}{2}+2} = (\lambda\bar{\lambda})^{\frac{|\mathcal{N}_{\mathcal{G}}|}{2}} [\delta^N(e)]^2, \quad (6)$$

and that the bound is optimal (that is there exist graphs at any order saturating it). In order to obtain a sensible large N limit, the scaling of the couplings λ and $\bar{\lambda}$ must be chosen such that the maximally divergent graphs have uniform degree of divergence at all orders.

III. RIBBON GRAPHS

To any CGFT graph one associates two classes of ribbon graphs: its bubbles [17] and its jackets [22]. We denote in the sequel $\widehat{i} = \{0, 1, 2, 3\} \setminus \{i\}$, $\widehat{ij} = \{0, 1, 2, 3\} \setminus \{i, j\}$ and $\widehat{ijk} = \{0, 1, 2, 3\} \setminus \{i, j, k\}$.

Bubbles. The bubbles [17] of a CGFT graph are the maximally connected subgraphs with three colors. They are dual to the vertices of the gluing of tetrahedra². The bubbles admit two representations, either as colored graphs or as ribbon graphs [17, 18]. The ribbon graph of a bubble with colors i, j, k is obtained by deleting all the strands containing the color \widehat{ijk} . The bubbles of the graph \mathcal{G}_1 (figure 2) are represented in figure 3. We denote $\mathcal{B}_{\mathcal{G}}$ the set of

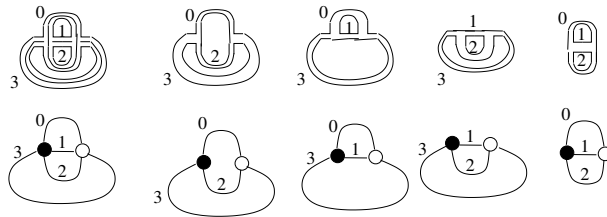


FIG. 3. The bubbles of \mathcal{G}_1 .

all the bubbles of \mathcal{G} and $\mathcal{B}_{\mathcal{G}}^{ijk}$ the set of bubbles of colors ijk .

For a bubble $b \in \mathcal{B}_{\mathcal{G}}$, we denote n_b , l_b and f_b the sets of its vertices, lines and faces. The graph \mathcal{G} has four valent vertices ($2|\mathcal{N}_{\mathcal{G}}| = |\mathcal{L}_{\mathcal{G}}|$), while its bubbles have three valent vertices ($3|n_b| = 2|l_b|$). We have

$$\begin{aligned} 4|\mathcal{N}_{\mathcal{G}}| &= \sum_{b \in \mathcal{B}_{\mathcal{G}}} |n_b|, & 3|\mathcal{L}_{\mathcal{G}}| &= \sum_{b \in \mathcal{B}_{\mathcal{G}}} |l_b|, & 2|\mathcal{F}_{\mathcal{G}}| &= \sum_{b \in \mathcal{B}_{\mathcal{G}}} |f_b|, \\ |\mathcal{N}_{\mathcal{G}}| - |\mathcal{L}_{\mathcal{G}}| + |\mathcal{F}_{\mathcal{G}}| - |\mathcal{B}_{\mathcal{G}}| &= - \sum_{b \in \mathcal{B}_{\mathcal{G}}} g_b, \end{aligned} \quad (7)$$

with g_b the genus of the bubble b . A graph \mathcal{G} is dual to an orientable pseudo manifold. If all its bubbles are planar then it is dual to an orientable manifold [14].

Jackets. A second class of ribbon graph associated to \mathcal{G} are its jackets [22]. A jacket of \mathcal{G} is the ribbon graph obtained from \mathcal{G} by deleting all the faces with colors ij and \widehat{ij} . A CGFT graph has three jackets. The three jackets of \mathcal{G}_1 are represented in figure 4, where the labels are associated to the faces.

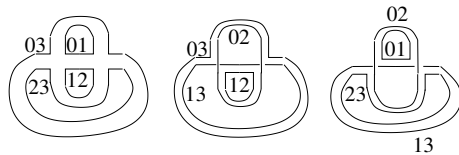


FIG. 4. The jackets of \mathcal{G}_1 .

The jackets of \mathcal{G} have four valent ribbon vertices. The reader might be worried that, while the vertices of the jacket with faces 02, 13 deleted (the one originally identified in [22]) are simple ribbon vertices, the ones of the other two jackets (with the faces 03, 12 and 01, 23 deleted) appear twisted in figure 4. This is just an illusion: permuting the half lines 0 and 1 and respectively 1 and 2 on every jacket vertex eliminates all the twists. The sets of vertices, lines and faces of a jacket are $\mathcal{N}_{\mathcal{G}}$, $\mathcal{L}_{\mathcal{G}}$ and $\mathcal{F}_{\mathcal{G}} \setminus \mathcal{F}_{\mathcal{G}}^{ij} \setminus \mathcal{F}_{\mathcal{G}}^{\widehat{ij}}$.

Face routing. In non identically distributed matrix models [27–29] the amplitude of a Feynman graph is computed via a “routing” algorithm, a digested version of which we present below.

² Recently an alternative definition for bubbles has been proposed in [26]. Although interesting in itself, this definition is somewhat idiosyncratic, and it seems preferable to use the more standard notion of bubbles dual to vertices of the gluing of tetrahedra.

To every ribbon graph \mathcal{H} (with sets of vertices, lines and faces denoted \mathcal{N} , \mathcal{L} and \mathcal{F}) one associates a dual graph $\tilde{\mathcal{H}}$. The construction is standard (see for instance [23, 29] and references therein). The vertices of \mathcal{H} , correspond to the faces of $\tilde{\mathcal{H}}$, its lines to the lines of $\tilde{\mathcal{H}}$ and its faces to the vertices of $\tilde{\mathcal{H}}$. The lines of \mathcal{H} admit (many) partitions in three disjoint sets: a tree \mathcal{T} in \mathcal{H} , ($|\mathcal{T}| = |\mathcal{N}| - 1$), a tree $\tilde{\mathcal{T}}$ in the its dual $\tilde{\mathcal{H}}$, ($|\tilde{\mathcal{T}}| = |\mathcal{F}| - 1$), and a set $\mathcal{L} \setminus \mathcal{T} \setminus \tilde{\mathcal{T}}$, ($|\mathcal{L} \setminus \mathcal{T} \setminus \tilde{\mathcal{T}}| = 2g_{\mathcal{H}}$) of “genus” lines ([23]).

We orient the faces of \mathcal{H} such that the two strands of every line have opposite orientations. We set a face of \mathcal{H} as “root” (denoted r). Consider a faces f sharing some line $l(f, \tilde{\mathcal{T}}) \in \tilde{\mathcal{T}}$ with the root (that is the two strands of $l(f, \tilde{\mathcal{T}})$ belong one to r and the other to f). The group element $h_{l(f, \tilde{\mathcal{T}})}$ appears exactly once in the argument of δ_f^N and δ_r^N

$$\delta_r^N \left(\prod_{\ell}^{\rightarrow} h_{\ell}^{\sigma^{\ell|r}} \right) \delta_f^N \left(\prod_{\ell}^{\rightarrow} h_{\ell}^{\sigma^{\ell|f}} \right) = \delta_r^N \left(\left(\prod_{\ell \neq l(f, \tilde{\mathcal{T}})}^{\rightarrow} h_{\ell}^{\sigma^{\ell|r}} \right) h_{l(f, \tilde{\mathcal{T}})}^{\sigma^{l(f, \tilde{\mathcal{T}})|r}} \right) \delta_f^N \left(h_{l(f, \tilde{\mathcal{T}})}^{\sigma^{l(f, \tilde{\mathcal{T}})|f}} \left(\prod_{\ell \neq l(f, \tilde{\mathcal{T}})}^{\rightarrow} h_{\ell}^{\sigma^{\ell|f}} \right) \right), \quad (8)$$

where we set $l(f, \tilde{\mathcal{T}})$ as the last line of r and as the first line of f . By our choice of orientations $\sigma^{l(f, \tilde{\mathcal{T}})|r} \sigma^{l(f, \tilde{\mathcal{T}})|f} = -1$ and eq. (8) becomes

$$\delta_r^N \left(\left(\prod_{\ell \neq l(f, \tilde{\mathcal{T}})}^{\rightarrow} h_{\ell}^{\sigma^{\ell|r}} \right) \left(\prod_{\ell \neq l(f, \tilde{\mathcal{T}})}^{\rightarrow} h_{\ell}^{\sigma^{\ell|f}} \right) \right) \delta_f^N \left(h_{l(f, \tilde{\mathcal{T}})}^{\sigma^{l(f, \tilde{\mathcal{T}})|f}} \left(\prod_{\ell \neq l(f, \tilde{\mathcal{T}})}^{\rightarrow} h_{\ell}^{\sigma^{\ell|f}} \right) \right). \quad (9)$$

This trivial multiplication has two consequences. First the face f is canonically associated to the line $l(f, \tilde{\mathcal{T}})$. Second, the face r becomes a root face in the graph $\mathcal{H} - l(f, \tilde{\mathcal{T}})$, obtained from \mathcal{H} by deleting $l(f, \tilde{\mathcal{T}})$ and connecting r and f into a new face $r' = r \cup f$ (see figure 5). Iterating for all faces except the root we get

$$\prod_{f \in \mathcal{H}} \delta_f^N \left(\prod_{\ell}^{\rightarrow} h_{\ell}^{\sigma^{\ell|f}} \right) = \delta_r^N \left(\prod_{\ell \notin \tilde{\mathcal{T}}}^{\rightarrow} h_{\ell}^{\sigma^{\ell| \cup_{f \in \mathcal{H}} f}} \right) \prod_{f \in \mathcal{H}, f \neq r} \delta_f^N \left(h_{l(f, \tilde{\mathcal{T}})}^{\sigma^{l(f, \tilde{\mathcal{T}})|f}} \left(\prod_{\ell \neq l(f, \tilde{\mathcal{T}})}^{\rightarrow} h_{\ell}^{\sigma^{\ell|f}} \right) \right). \quad (10)$$

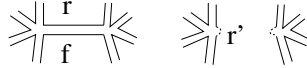


FIG. 5. Deletion of a ribbon line.

If \mathcal{H} is planar, $\cup_{f \in \mathcal{H}} f$ is the exterior face of the tree \mathcal{T} in \mathcal{H} . The group elements corresponding to lines of \mathcal{T} touching leaves (vertices of coordination one in \mathcal{T}) appear consecutively $h_l h_l^{-1}$, and drop from the root face. Iterating for all line in \mathcal{T} we get

$$\delta_r^N \left(\prod_{\ell \notin \tilde{\mathcal{T}}}^{\rightarrow} h_{\ell}^{\sigma^{\ell| \cup_{f \in \mathcal{H}} f}} \right) \Big|_{\mathcal{H} \text{ planar}} = \delta^N(e), \quad (11)$$

for *any* base group G . Remark that only the argument of the root δ_r^N changes under routing.

An Example: 2D GFT. The 2 dimensional GFT (with $G = SU(2)$) is a non identically distributed matrix model. The couplings do not need to be rescaled in this case. The free energy admits a familiar “genus expansion”.

By face routing one can integrate all group elements h_l with $l \in \tilde{\mathcal{T}}$ and by a tree change of variables [19] one eliminates all group elements h_l with $l \in \mathcal{T}$. One is left with an integral over the genus lines corresponding to a “super rosette graph” [23] with only one vertex and one face. The super rosette is obtained from \mathcal{G} by deleting the lines in $\tilde{\mathcal{T}}$ and contracting the lines in \mathcal{T} . The particular super rosette to which a graph is reduced depends on the routing trees \mathcal{T} and $\tilde{\mathcal{T}}$, but all super rosettes associated to a graph have the same genus g . One can define $[R_g]$ as the equivalence class of all super rosettes of genus g . For a super rosette, each genus line appears twice in the argument of the last δ^N function. We expand in characters and integrate the genus lines (by the “third Filk move” in the dual super rosette [23]). Each genus line brings a factor $(2j+1)^{-1}$, hence the amplitude of a super rosette is $A^{R_g} = \sum (2j+1)^{1-2g} \approx N^{2-2g}$, for all super rosettes of genus g ³. The amplitude of \mathcal{G} equals the one of the super rosette class to which it belongs. The genus expansion of the free energy writes

$$F(\lambda, \bar{\lambda}) = \sum C^{[R_g]}(\lambda, \bar{\lambda}) A^{[R_g]} = \sum C^{[R_g]}(\lambda, \bar{\lambda}) N^{2-2g}, \quad (12)$$

³ To correctly identify the scaling with N one must use sliced δ^N functions, $\delta^N(h) = \sum_{N/2}^N (2j+1) \chi^j(h)$.

with $C^{[R_g]}(\lambda, \bar{\lambda})$ a combinatorial factor counting the graphs which reduce to the super rosette class $[R_g]$ i.e. all graphs of genus g . Of course in 2 dimensions, as the super rosette amplitudes can be computed explicitly one completely forgets about them, indexes the expansion of the free energy by the genus g and concludes that higher and higher genus graphs are suppressed by larger and larger powers of the cut off.

IV. DIPOLES

The second ingredient we need to establish our results are the Dipole moves [24, 25] encoding homeomorphisms of pseudo manifolds (we will make a precise statement later). We will identify the various bubbles, faces and lines below by their colors (in superscript) and their vertices (in subscript).

1-Dipoles. Consider a line of color 3 with end vertices v and w (denoted L_{vw}^3) in a graph \mathcal{G} . Call a_0 (a_1 and a_2) the end vertex of the line of color 0 (1 and 2) touching v , and b_0 (b_1 and b_2) the end vertex of the line of color 0 (1 and 2) touching w (see figure 6). The vertices v and w belong each to some 3-bubble of colors 012, $B_{va_0a_1a_2}^{012}$ and $B_{wb_0b_1b_2}^{012}$. The two bubbles might coincide or might be different. If they are different and at least one of them is planar then the line L_{vw}^3 is called an *1-Dipole*.

A 1-Dipole can be contracted, that is the line L_{vw}^3 together with the vertices v and w can be deleted from the graph and the remaining lines reconnected *respecting the coloring* (see figure 6). In the dual gluing a 1-Dipole of color 3 represents two tetrahedra sharing the triangle (of color 3) such that the vertices opposite to the triangle (duals to $B_{va_0a_1a_2}^{012}$ and $B_{wb_0b_1b_2}^{012}$) are different. The contraction translates in squashing the two tetrahedra, merging the two vertices, and coherently identifying the remaining triangles 0, 1 and 2 (see figure 6).

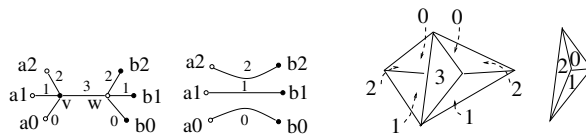


FIG. 6. 1-Dipole contraction in \mathcal{G} and its dual gluing.

In this picture it is clear why one of $B_{va_0a_1a_2}^{012}$ or $B_{wb_0b_1b_2}^{012}$ is required to be planar. If both points opposite to the triangle 3 were isolate singularities, the squashing of tetrahedra would decrease the number of singular points and would not be a homeomorphism. It is however a homeomorphism as long as one of the points is regular⁴.

The vertices v and w belong to *the same* faces 03, 13 and 23 ($F_{vwa_0b_0}^{03}$, $F_{vwa_1b_1}^{13}$, $F_{vwa_2b_2}^{23}$), but *distinct* faces 01, 02 and 12 ($F_{va_0a_1}^{01}$, $F_{wb_0b_1}^{01}$, $F_{va_0a_2}^{02}$, $F_{wb_0b_2}^{02}$ and $F_{va_1a_2}^{12}$, $F_{wb_1b_2}^{12}$). They also belong to *the same* bubbles 013, 023 and 123, ($B_{vwa_0a_1b_0b_1}^{013}$, $B_{vwa_0a_2b_0b_2}^{023}$, $B_{vwa_1a_2b_1b_2}^{123}$) but *different* bubbles 012 ($B_{va_0a_1a_2}^{012}$ and $B_{wb_0b_1b_2}^{012}$). We track the effect of the 1-Dipole contraction on the graph \mathcal{G} . Taking $B_{va_0a_1a_2}^{012}$ the planar bubble, the contraction

- deletes the vertices v and w and the line L_{vw}^3 .
- glues $L_{va_0}^0$ on $L_{wb_0}^0$ to form a new line L_{vw}^0 (and similarly for colors 1 and 2).
- transforms the face $F_{vwa_0b_0}^{03}$ into a face $F_{a_0b_0}^{03}$ (and similarly for 13 and 23) .
- glues the face $F_{va_0a_1}^{01}$ on the face $F_{wb_0b_1}^{01}$ to form a new face $F_{a_0b_0b_1a_1}^{01}$ (and similarly for 02 and 12).
- transforms the bubble $B_{vwa_0a_1b_0b_1}^{013}$ into a bubble $B_{a_0a_1b_0b_1}^{013}$ (and similarly for 023 and 123)
- glues $B_{va_0a_1a_2}^{012}$ on $B_{wb_0b_1b_2}^{012}$ to form a new bubble $B_{a_0b_0a_1b_1a_2b_2}^{012}$.

The bubbles 013, 023 and 123 transform trivially under contraction. Call n, l, f and g (n', l', f' and g') the vertices, lines, faces and genus of one of these bubbles before (after) contraction. We have

$$|n'| = |n| - 2, \quad |l'| = |l| - 3, \quad |f'| = |f| - 1 \Rightarrow g' = g. \quad (13)$$

⁴ See [25], especially the remark on page 93 in the proof of the main theorem.

The bubble $B_{va_0a_1a_2}^{012}$ (with n_a, l_a, f_a and g_a) is glued on $B_{wb_0b_1b_2}^{012}$ (with n_b, l_b, f_b and g_b) to form the new bubble $B_{a_0b_0a_1b_1a_2b_2}^{012}$ (with n'_b, l'_b, f'_b and g'_b) and

$$|n'_b| = |n_a| + |n_b| - 2, \quad |l'_b| = |l_a| + |l_b| - 3, \quad |f'_b| = |f_a| + |f_b| - 3 \Rightarrow g'_b = g_a + g_b. \quad (14)$$

Thus $g'_b = g_b$ if $g_a = 0$. If $B_{wb_0b_1b_2}^{012}$ is dual to a conical singularity ($g_b \neq 0$) then the new bubble $B_{a_0b_0a_1b_1a_2b_2}^{012}$ is dual to an identical singularity and the two dual pseudo manifolds are homeomorphic [25]. Were we to allow a contraction when both $g_a, g_b \neq 0$ we would merge two conical singularities into a unique (more degenerate) conical singularity.

Amplitude. Suppose that all lines enter v and exit w . We denote $h_{0;v}$ the group element associated to $L_{va_0}^0$, etc. and use the shorthand notation $(01);v$ for $F_{va_0a_1}^{01}$ etc. The contribution of all faces containing v and/or w to the amplitude of \mathcal{G} is

$$\begin{aligned} & \int dh_{0;v} dh_{0;w} dh_{1;v} dh_{1;w} dh_{2;v} dh_{2;w} dh_3 \\ & \delta_{(03)}^N(h_{0;v} h_3^{-1} h_{0;w} f^{03}) \delta_{(13)}^N(h_{1;v} h_3^{-1} h_{1;w} f^{13}) \delta_{(23)}^N(h_{2;v} h_3^{-1} h_{2;w} f^{23}) \\ & \delta_{(01);v}^N(h_{0;v} h_{1;v}^{-1} f_v^{01}) \delta_{(02);v}^N(h_{2;v} h_{0;v}^{-1} f_v^{02}) \delta_{(12);v}^N(h_{1;v} h_{2;v}^{-1} f_v^{12}) \\ & \delta_{(01);w}^N(h_{1;w}^{-1} h_{0;w} f_w^{01}) \delta_{(02);w}^N(h_{0;w}^{-1} h_{2;w} f_w^{02}) \delta_{(12);w}^N(h_{2;w}^{-1} h_{1;w} f_w^{12}), \end{aligned} \quad (15)$$

where f^{03} denotes the product of the remaining group elements along the face 03 and similarly for the rest. We first change variables to $h'_{0;w} = h_3^{-1} h_{0;w}$, $dh'_{0;w} = dh_{0;w}$ (and similarly for $h_{1;w}$ and $h_{2;w}$). The integral over h_3 is trivial. Forgetting the primes we obtain

$$\begin{aligned} & \int dh_{0;v} dh_{0;w} dh_{1;v} dh_{1;w} dh_{2;v} dh_{2;w} \\ & \delta_{(03)}^N(h_{0;v} h_{0;w} f^{03}) \delta_{(13)}^N(h_{1;v} h_{1;w} f^{13}) \delta_{(23)}^N(h_{2;v} h_{2;w} f^{23}) \\ & \delta_{(01);v}^N(h_{0;v} h_{1;v}^{-1} f_v^{01}) \delta_{(02);v}^N(h_{2;v} h_{0;v}^{-1} f_v^{02}) \delta_{(12);v}^N(h_{1;v} h_{2;v}^{-1} f_v^{12}) \\ & \delta_{(01);w}^N(h_{1;w}^{-1} h_{0;w} f_w^{01}) \delta_{(02);w}^N(h_{0;w}^{-1} h_{2;w} f_w^{02}) \delta_{(12);w}^N(h_{2;w}^{-1} h_{1;w} f_w^{12}). \end{aligned} \quad (16)$$

We change again variables to $h_0 = h_{0;v} h_{0;w}$, $dh_0 = h_{0;w}$ (and similarly for $h_{1;w}$ and $h_{2;w}$) to obtain

$$\begin{aligned} & \int dh_{0;v} dh_0 dh_{1;v} dh_1 dh_{2;v} dh_2 \\ & \delta_{(03)}^N(h_0 f^{03}) \delta_{(13)}^N(h_1 f^{13}) \delta_{(23)}^N(h_2 f^{23}) \\ & \delta_{(01);v}^N(h_{0;v} h_{1;v}^{-1} f_v^{01}) \delta_{(02);v}^N(h_{2;v} h_{0;v}^{-1} f_v^{02}) \delta_{(12);v}^N(h_{1;v} h_{2;v}^{-1} f_v^{12}) \\ & \delta_{(01);w}^N(h_1^{-1} h_{1;v} h_{0;v}^{-1} f_w^{01}) \delta_{(02);w}^N(h_0^{-1} h_{0;v} h_{2;v}^{-1} f_w^{02}) \delta_{(12);w}^N(h_2^{-1} h_{2;v} h_{1;v}^{-1} f_w^{12}). \end{aligned} \quad (17)$$

We integrate $h_{1;v}, h_{2;v}$ using $\delta_{(01);v}^N$ and $\delta_{(02);v}^N$ (hence $h_{1;v} = f_v^{01} h_{0;v}$, $h_{2;v} = h_{0;v}^{-1} f_v^{02}$) and eq. (15) becomes

$$\begin{aligned} & \int dh_{0;v} dh_0 dh_1 dh_2 \\ & \delta_{(03)}^N(h_0 f^{03}) \delta_{(13)}^N(h_1 f^{13}) \delta_{(23)}^N(h_2 f^{23}) \\ & \delta_{(12);v}^N(f_v^{01} f_v^{02} f_v^{12}) \\ & \delta_{(01);w}^N(h_1^{-1} f_v^{01} h_0 f_w^{01}) \delta_{(02);w}^N(h_0^{-1} f_v^{02} h_2 f_w^{02}) \delta_{(12);w}^N(h_2^{-1} f_v^{12} h_1 f_w^{12}). \end{aligned} \quad (18)$$

Remark that, ignoring $\delta_{(12);v}^N$, the integrand of eq. (18) corresponds to the graph with the 1-Dipole contracted. But $\delta_{(12);v}^N$ reproduces the external face of a ribbon graph obtained by cutting the vertex v in the bubble $B_{va_0a_1a_2}^{012}$. The latter is a planar ribbon graph hence by eq. (11) $\delta_{(12);v}^N(f_v^{01} f_v^{02} f_v^{12})$ can be replaced by $\delta^N(e)$. Recalling that the number of vertices decreases by 2 we obtain that the amplitudes of \mathcal{G} and $\mathcal{G} - L_{vw}^3$ (the graph with the 1-Dipole L_{vw}^3 contracted), are proportional

$$A^{\mathcal{G}} = \frac{(\lambda \bar{\lambda})}{\delta^N(e)} \delta^N(e) A^{\mathcal{G} - L_{vw}^3} = (\lambda \bar{\lambda}) A^{\mathcal{G} - L_{vw}^3}. \quad (19)$$

2-Dipoles. A *2-Dipole* of colors 23 (see figure 7) is a couple of lines connecting the same two vertices v and w , L_{vw}^2 and L_{vw}^3 such that the faces $F_{va_0a_1}^{01}$ and $F_{wb_0b_1}^{01}$ are different. The 2-Dipole forms a face F_{vw}^{23} . Like the 1-Dipoles, the 2-Dipoles can be contracted (by deleting the lines 2 and 3 forming the 2-Dipole and reconnecting the rest of the

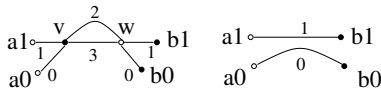


FIG. 7. 2-Dipole contraction.

lines respecting the colors). This is represented in figure 7. After contraction the two faces $F_{va_0a_1}^{01}$ and $F_{wb_0b_1}^{01}$ are glued into a unique face $F_{a_0a_1b_0b_1}^{01}$. A 2-Dipole is dual to two tetrahedra sharing two triangles (of colors 2 and 3 for figure 7) such that the edge opposite to the two triangles in each tetrahedron (dual to the faces $F_{va_0a_1}^{01}$ and $F_{wb_0b_1}^{01}$) are different. The contraction translates in squashing the two tetrahedra and coherently identifying the remaining boundary triangles. This move always represents a homeomorphism [25]. Denoting $\mathcal{G} - F_{vw}^{23}$ the graph obtained from \mathcal{G} after contracting the 2-Dipole, a short computation along the lines of the one for 1-Dipoles yields

$$A^{\mathcal{G}} = \frac{(\lambda\bar{\lambda})}{\delta^N(e)} A^{\mathcal{G} - F_{vw}^{23}}. \quad (20)$$

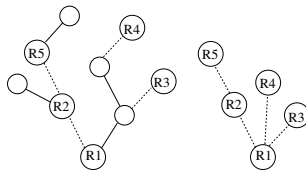
The Dipole contraction moves can be inverted into Dipole creation moves. The fundamental result we will use in the sequel [25] is that two pseudo manifolds dual to colored graphs \mathcal{G} and \mathcal{G}' are homeomorphic if \mathcal{G} and \mathcal{G}' are related by a finite sequence of 1 and 2-Dipole creation and contraction moves. We call two such graphs “equivalent”, $\mathcal{G} \sim \mathcal{G}'$.

V. BUBBLE ROUTING AND CORE GRAPHS

In the literature one finds two classes of results (bounds and evaluations) for amplitudes of GFT graphs. They are expressed either in terms of the number of vertices ([20, 21]) or in terms of the number of bubbles [19, 22]. In order to build the $1/N$ expansion in CGFT we need to strike the right balance between the vertices and the bubbles of a graph. This is achieved by a bubble routing algorithm.

Bubble routing. We start by choosing a set of roots of \mathcal{G} for all colors i . For the color 3, if all the bubbles \mathcal{B}^{012} are planar we chose one of them as root and denote it R_1^{012} . If there exist non planar bubbles 012 we set a non planar bubble as principal root R_1^{012} , and the other non planar bubbles as “branch roots” $R_2^{012}, R_3^{012}, \dots$. We denote the set of 012 roots of \mathcal{G} by $\mathcal{R}^{012} = \{R_1^{012}, R_2^{012}, \dots\}$. We repeat this for all colors (and denote $\mathcal{R}_{\mathcal{G}}$ the set of all roots of \mathcal{G}).

We associate to the bubbles 012 of \mathcal{G} a “012 connectivity graph”. Its vertices represent the various bubbles 012. Its lines are the lines of color 3 in \mathcal{G} . They either start and end on the same bubble 012 (in which case they are “tadpole” lines in the connectivity graph), or not. A particularly simple way to picture the 012 connectivity graph is to draw \mathcal{G} with lines 0, 1 and 2 much shorter than the lines 3. We chose a tree in the connectivity graph, \mathcal{T}^3 (and call the rest of the lines 3 “loop lines”). For a branch root R_q^{012} , the line incident on it and belonging to the path in \mathcal{T}^3 connecting R_q^{012} to the principal root R_1^{012} is represented as dashed. All the other lines in \mathcal{T}^3 are represented as solid lines. An example is given in figure 8.

FIG. 8. A tree \mathcal{T}^3 in the 012 connectivity graph.

All the solid lines in \mathcal{T}^3 are 1-Dipoles and we contract them. We end up with a connectivity graph with vertices corresponding to the roots R_q^{012} . The remaining lines of color 3 cannot be 1-Dipoles (they are either tadpole lines or they separate two non planar roots). The number of 1-Dipoles of color 3 contracted is $|\mathcal{B}^{012}| - |\mathcal{R}^{012}|$. Neither the number nor the topology of the bubbles of the other colors, \mathcal{B}^{013} , \mathcal{B}^{023} and \mathcal{B}^{123} is changed under these contractions.

Having exhausted a complete set of 1-Dipoles of color 3, we repeat the procedure for the 1-Dipoles of color 2. The routing tree \mathcal{T}^2 is chosen in the graph obtained *after* contracting the 1-Dipoles of color 3 and depends on \mathcal{T}^3 , $\mathcal{T}^2(\mathcal{T}^3)$. The contraction of 1-Dipole of color 2 changes the 012 connectivity graph but it *cannot* create new 1-Dipoles of color

3: the topology of the 012 bubbles is unaffected by reducing 1-Dipoles of color 2, hence the lines of color 3 will still either be tadpole lines or separate two non planar roots 012. After a full set of 1-Dipole contractions indexed by four distinct routing trees $\mathcal{T}^3, \mathcal{T}^2(\mathcal{T}^3), \mathcal{T}^1(\mathcal{T}^2, \mathcal{T}^3), \mathcal{T}^0(\mathcal{T}^1, \mathcal{T}^2, \mathcal{T}^3)$ we obtain a *Core Graph*⁵.

Definition 1 (Core Graph). A colored graph with $2p$ vertices \mathcal{G}_p is called a *Core Graph* at order p if, for all colors i , it either has a unique (planar or non planar) bubble $P_1^{\hat{i}}$ or all its bubbles $P_1^{\hat{i}}, P_2^{\hat{i}}, \dots$ are non planar.

The amplitude of the graph \mathcal{G} and of the Core Graph obtained after routing are related by

$$A^{\mathcal{G}} = (\lambda\bar{\lambda})^{|\mathcal{B}_{\mathcal{G}}| - |\mathcal{R}_{\mathcal{G}}|} A^{\mathcal{G}_p}, \quad 2p = |\mathcal{N}_{\mathcal{G}}| - 2(|\mathcal{B}_{\mathcal{G}}| - |\mathcal{R}_{\mathcal{G}}|). \quad (21)$$

The Core Graph one obtains by routing is *not* independent of the routing trees $\mathcal{T}^3, \mathcal{T}^2, \mathcal{T}^1, \mathcal{T}^0$. The same graph leads to several equivalent Core Graphs, all at the same order p , $\mathcal{G}_p \sim \mathcal{G}'_p \sim \dots$. One can prove that all equivalent Core Graphs at the same order $\mathcal{G}_p \sim \mathcal{G}'_p$ have the same amplitude. Only the creation/contraction of dipoles of color i can change the number of bubbles of colors \hat{i} , and the latter only create/annihilate planar bubbles. It follows that the numbers of bubbles of colors \hat{i} of \mathcal{G}_p and \mathcal{G}'_p are equal and consequently the total numbers of 1-Dipole creations and contractions are equal. As \mathcal{G}_p and \mathcal{G}'_p have the same number of vertices, the total numbers of 2-Dipole creations and contractions are also equal and $A^{\mathcal{G}_p} = A^{\mathcal{G}'_p}$.

We denote $\mathfrak{G}_p = \{[\mathcal{G}_p]\}$ the set of equivalence classes of Core Graphs at order p under the equivalence relation \sim . The amplitude is a well defined function of the equivalence class $[\mathcal{G}_p]$. Under an arbitrary routing any graph will fall in a unique equivalence class $[\mathcal{G}_p]$. The free energy of the colored Boulatov model admits a topological expansion in Core Graphs classes

$$F(\lambda, \bar{\lambda}) = \sum_{p=1}^{\infty} \sum_{[\mathcal{G}_p] \in \mathfrak{G}_p} C^{[\mathcal{G}_p]}(\lambda, \bar{\lambda}) A^{[\mathcal{G}_p]}, \quad (22)$$

where $C^{[\mathcal{G}_p]}(\lambda, \bar{\lambda})$ is a combinatorial factor counting all the graphs routing to a Core Graph class at order p . The scaling with N is entirely captured by the Core Graph amplitude $A^{[\mathcal{G}_p]}$. A Core Graphs class is dual to a specific pseudo manifold. Note however that the same pseudo manifold is represented by an infinity of classes $[\mathcal{G}_p]$ at higher and higher orders in p .

Core Graphs are in three dimensions the appropriate generalization of the super rosettes of two dimensional GFT. The only ingredient missing at this point is some estimate of their amplitude.

Theorem 1 (The Core Graph bound). The amplitude of a Core Graph at order p , \mathcal{G}_p , with set of bubble \mathcal{P} respects

$$|A^{\mathcal{G}_p}| \leq (\lambda\bar{\lambda})^p [\delta^N(e)]^{-\frac{1}{3}p + \frac{1}{3} \sum_{b \in \mathcal{P}} (1 - g_b) + 1}. \quad (23)$$

Proof: We denote the set of lines and faces of \mathcal{G}_p by \mathcal{L} and \mathcal{F} . The amplitude of the Core Graph is

$$A^{\mathcal{G}_p} = \frac{(\lambda\bar{\lambda})^p}{[\delta^N(e)]^p} \int \prod_{\ell \in \mathcal{L}} dh_{\ell} \prod_{f \in \mathcal{F}} \delta_f^N \left(\prod_{\ell \in f} h_{\ell}^{\sigma_{\ell f}} \right). \quad (24)$$

Denote \mathcal{J}^{ij} the jacket of \mathcal{G}_p with the faces faces ij and \hat{ij} deleted. The idea is to use the jacket graph to integrate explicitly as many group elements as possible. Indeed, routing the faces of the jacket graph will associate a line to all (save one) of its faces. When integrating all (save one) of the δ^N functions of the faces of the jacket graph will contribute 1, as $\int dh \delta^N(h^{-1} \dots) K(h) = K(\dots)$. The effect of this integrations over the rest of the δ^N functions is exceedingly complicated to track. However we will not need to do it, as we will just use a naive bound $\delta^N(h) \leq \delta^N(e)$ for all of them. In detail

$$A^{\mathcal{G}_p} = \frac{(\lambda\bar{\lambda})^p}{[\delta^N(e)]^p} \int \prod_{\ell \in \mathcal{L}} dh_{\ell} \left[\prod_{f' \in \mathcal{F}^{ij} \cup \mathcal{F}^{\hat{ij}}} \delta_{f'}^N \left(\prod_{\ell \in f'} h_{\ell}^{\sigma_{\ell f'}} \right) \right] \left[\prod_{f \in \mathcal{J}^{ij}} \delta_f^N \left(\prod_{\ell \in f} h_{\ell}^{\sigma_{\ell f}} \right) \right], \quad (25)$$

and routing the faces of the jacket graph via a tree $\tilde{\mathcal{T}}$ in the dual graph of the jacket we get

$$A^{\mathcal{G}_p} = \frac{(\lambda\bar{\lambda})^p}{[\delta^N(e)]^p} \int \prod_{\ell \in \mathcal{L}_p} dh_{\ell} \left[\prod_{f' \in \mathcal{F}^{ij} \cup \mathcal{F}^{\hat{ij}}} \delta_{f'}^N \left(\prod_{\ell \in f'} h_{\ell}^{\sigma_{\ell f'}} \right) \right]$$

⁵ If \mathcal{G} is dual to a manifold and one further reduces a full set of 2-Dipoles one recovers a ‘‘gem’’ graph of [24].

$$\left[\delta_r^N \left(\prod_{\ell \notin \tilde{\mathcal{T}}}^{\rightarrow} h_\ell^{\sigma^{\ell \cup f \in \mathcal{J}^{ij} f}} \right) \prod_{f \in \mathcal{J}^{ij}, f \neq r} \delta_f^N \left(h_{l(f, \tilde{\mathcal{T}})}^{\sigma^{l(f, \tilde{\mathcal{T}}) | f}} \left(\prod_{\ell \neq l(f, \tilde{\mathcal{T}})}^{\rightarrow} h_\ell^{\sigma^{\ell | f}} \right) \right) \right]. \quad (26)$$

Each of the δ^N of the faces of the jacket can now be associated uniquely to a specific integral over some group element. For all the lines in $\tilde{\mathcal{T}}$ we change variables to

$$\tilde{h}_{l(f, \tilde{\mathcal{T}})} = h_{l(f, \tilde{\mathcal{T}})}^{\sigma^{l(f, \tilde{\mathcal{T}}) | f}} \left(\prod_{\ell \neq l(f, \tilde{\mathcal{T}})}^{\rightarrow} h_\ell^{\sigma^{\ell | f}} \right), \quad (27)$$

and write (in sloppy notations)

$$A^{\mathcal{G}_p} = \frac{(\lambda \bar{\lambda})^p}{[\delta^N(e)]^p} \int \prod_{\ell \in \mathcal{L}_p \setminus \tilde{\mathcal{T}}} dh_\ell \prod_{l \in \tilde{\mathcal{T}}} d\tilde{h}_l \left[\prod_{f' \in \mathcal{F}_p^{ij} \cup \mathcal{F}_p^{\widehat{ij}}} \delta_{f'}^N(\dots) \right] \delta_r^N(\dots) \left[\prod_{f \in \mathcal{J}^{ij}, f \neq r} \delta_f^N(\tilde{h}_{l(f, \tilde{\mathcal{T}})}) \right]. \quad (28)$$

Each δ^N in the last line integrates with its associated $\tilde{h}_{l(f, \tilde{\mathcal{T}})}$, and we get

$$A^{\mathcal{G}_p} = \frac{(\lambda \bar{\lambda})^p}{[\delta^N(e)]^p} \int \prod_{\ell \in \mathcal{L}_p \setminus \tilde{\mathcal{T}}} dh_\ell \left[\prod_{f' \in \mathcal{F}_p^{ij} \cup \mathcal{F}_p^{\widehat{ij}}} \delta_{f'}^N(\dots) \right] \delta_r^N(\dots) \leq \frac{(\lambda \bar{\lambda})^p}{[\delta^N(e)]^p} [\delta^N(e)]^{|\mathcal{F}^{ij}| + |\mathcal{F}^{\widehat{ij}}| + 1}. \quad (29)$$

One can use any of the three jackets of the graph to derive a bound. Using the jacket which yields the best estimate we always have

$$A^{\mathcal{G}_p} \leq \frac{(\lambda \bar{\lambda})^p}{[\delta^N(e)]^p} [\delta^N(e)]^{\frac{|\mathcal{F}|}{3} + 1}, \quad (30)$$

and by eq. (7) we have

$$2p - 4p + |\mathcal{F}| - |\mathcal{P}| = - \sum_{b \in \mathcal{P}} g_b \Rightarrow |\mathcal{F}| = 2p + \sum_{b \in \mathcal{P}} (1 - g_b). \quad (31)$$

□

Note that $\sum_{b \in \mathcal{P}} (1 - g_b) \leq 4$ (and equal 4 if and only if the Core Graph is dual to a manifold). The Core Graph bound ensures that more and more complicated topologies (i.e. topologies which cannot be represented by a Core Graph with p vertices or less) are suppressed at least as $[\delta^N(e)]^{\frac{7-p}{3}}$ in eq. (22).

The $1/N$ expansion. We are now in the position to perform the $1/N$ expansion of the colored GFT model. In order to evaluate all contributions to the order $[\delta^N(e)]^{-\alpha}$ one lists all (equivalence classes of) Core Graphs up to order $p = 3\alpha + 7$. This is a finite problem, hence solvable. Then one computes the amplitude of each Core Graph (which can of course turn out to be much smaller than the value predicted by the Core Graph bound). The free energy is

$$F(\lambda, \bar{\lambda}) = \sum_{p=1}^{3\alpha+7} \sum_{[\mathcal{G}_p] \in \mathfrak{G}_p} C^{[\mathcal{G}_p]}(\lambda, \bar{\lambda}) A^{[\mathcal{G}_p]} + O([\delta^N(e)]^{-\alpha}). \quad (32)$$

The Core Graphs graphs up to $p = 3$ are the graphs \mathcal{G}_1 , \mathcal{G}_2 , $\mathcal{G}_{3,a}$, $\mathcal{G}_{3,b}$, $\mathcal{G}_{3,c}$ and $\mathcal{G}_{3,d}$ from figure 2. The Core Graphs \mathcal{G}_1 , \mathcal{G}_2 , $\mathcal{G}_{3,a}$ and $\mathcal{G}_{3,b}$ are dual to the three sphere S^3 . The Core Graphs $\mathcal{G}_{3,a}$ and $\mathcal{G}_{3,b}$ are in the same equivalence class at order 3. The Core Graphs $\mathcal{G}_{3,c}$ and $\mathcal{G}_{3,d}$ are dual to pseudo manifolds: $\mathcal{G}_{3,c}$ has two non planar bubbles each of genus 1, while $\mathcal{G}_{3,d}$ has only one non planar bubble of genus 1. The Core Graph bound ensures that

$$\begin{aligned} A^{[\mathcal{G}_1]} &\leq [\delta^N(e)]^2, & A^{[\mathcal{G}_2]} &\leq [\delta^N(e)]^{\frac{5}{3}}, & A^{[\mathcal{G}_{3,a}]} &\leq [\delta^N(e)]^{\frac{4}{3}}, \\ A^{[\mathcal{G}_{3,c}]} &\leq [\delta^N(e)]^{\frac{2}{3}}, & A^{[\mathcal{G}_{3,d}]} &\leq [\delta^N(e)]. \end{aligned} \quad (33)$$

Contributions coming from Core Graphs at higher order are at most of order $\delta^N(e)$. Direct computation shows that

$$\begin{aligned} A^{[\mathcal{G}_1]} &= [\delta^N(e)]^2, & A^{[\mathcal{G}_2]} &= [\delta^N(e)], & A^{[\mathcal{G}_{3,a}]} &= [\delta^N(e)]^0, \\ A^{[\mathcal{G}_{3,c}]} &= \frac{1}{\delta^N(e)} \int dhdu \delta^N(hu^{-1}h^{-1}u), & A^{[\mathcal{G}_{3,d}]} &= [\delta^N(e)]^0. \end{aligned} \quad (34)$$

Hence the partition function of the colored Boulatov model develops as

$$F(\lambda, \bar{\lambda}) = C^{[\mathcal{G}_1]}(\lambda, \bar{\lambda}) [\delta^N(e)]^2 + O([\delta^N(e)]), \quad (35)$$

and all graphs contributing to the dominant order are dual to manifolds homeomorphic with the three sphere S^3 .

ACKNOWLEDGEMENTS

Research at Perimeter Institute is supported by the Government of Canada through Industry Canada and by the Province of Ontario through the Ministry of Research and Innovation.

-
- [1] L. Freidel, *Int. J. Theor. Phys.* **44**, 1769 (2005) [arXiv:hep-th/0505016].
 - [2] D. Oriti, [arXiv:0912.2441 [hep-th]].
 - [3] F. David, *Nucl. Phys. B* **257**, 543 (1985).
 - [4] M. Gross, *Nucl. Phys. Proc. Suppl.* **25A**, 144 (1992).
 - [5] J. Ambjorn, B. Durhuus and T. Jonsson, *Mod. Phys. Lett. A* **6**, 1133 (1991).
 - [6] N. Sasakura, *Mod. Phys. Lett. A* **6**, 2613 (1991).
 - [7] D. V. Boulatov, *Mod. Phys. Lett. A* **7**, 1629 (1992) [arXiv:hep-th/9202074].
 - [8] L. Freidel and D. Louapre, *Class. Quant. Grav.* **21**, 5685 (2004) [arXiv:hep-th/0401076].
 - [9] A. Baratin and D. Oriti, [arXiv:1002.4723 [hep-th]].
 - [10] J. Engle, R. Pereira and C. Rovelli, *Nucl. Phys. B* **798**, 251 (2008) [arXiv:0708.1236 [gr-qc]].
 - [11] E. R. Livine and S. Speziale, *Phys. Rev. D* **76**, 084028 (2007) [arXiv:0705.0674 [gr-qc]].
 - [12] L. Freidel and K. Krasnov, *Class. Quant. Grav.* **25**, 125018 (2008) [arXiv:0708.1595 [gr-qc]].
 - [13] J. B. Geloun, R. Gurau and V. Rivasseau, arXiv:1008.0354 [hep-th].
 - [14] R. Gurau, *Class. Quant. Grav.* **27**, 235023 (2010) arXiv:1006.0714 [hep-th].
 - [15] E. Brezin, C. Itzykson, G. Parisi and J. B. Zuber *Commun. Math. Phys.* **59**, 35 (1978).
 - [16] S. Alexandrov and P. Roche, arXiv:1009.4475 [gr-qc].
 - [17] R. Gurau, [arXiv:0907.2582 [hep-th]].
 - [18] R. Gurau, *Annales Henri Poincare* **11**, 565 (2010) [arXiv:0911.1945 [hep-th]].
 - [19] L. Freidel, R. Gurau and D. Oriti, *Phys. Rev. D* **80**, 044007 (2009) [arXiv:0905.3772 [hep-th]].
 - [20] J. Magnen, K. Noui, V. Rivasseau and M. Smerlak, *Class. Quant. Grav.* **26**, 185012 (2009) [arXiv:0906.5477 [hep-th]].
 - [21] J. B. Geloun, J. Magnen and V. Rivasseau, [arXiv:0911.1719 [hep-th]].
 - [22] J. B. Geloun, T. Krajewski, J. Magnen and V. Rivasseau, *Class. Quant. Grav.* **27**, 155012 (2010) [arXiv:1002.3592 [hep-th]].
 - [23] R. Gurau and V. Rivasseau, *Commun. Math. Phys.* **272**, 811 (2007) [arXiv:math-ph/0606030].
 - [24] S. Lins, *Gems, Computers and Attractors for 3-Manifolds, (Series on Knots and Everything, Vol 5)* ISBN: 9810219075/ ISBN-13: 9789810219079
 - [25] M. Ferri and C. Gagliardi *Pacific Journal of Mathematics* Vol. 100, No. 1, 1982
 - [26] V. Bonzom and M. Smerlak, *Lett. Math. Phys.* **93**, 295 (2010) [arXiv:1004.5196 [gr-qc]].
 - [27] H. Grosse and R. Wulkenhaar, *Commun. Math. Phys.* **256**, 305 (2005) [arXiv:hep-th/0401128].
 - [28] R. Gurau, J. Magnen, V. Rivasseau and F. Vignes-Tourneret, *Commun. Math. Phys.* **267**, 515 (2006) [arXiv:hep-th/0512271].
 - [29] V. Rivasseau, F. Vignes-Tourneret, R. Wulkenhaar, *Commun. Math. Phys.* **262**, 565-594 (2006). [hep-th/0501036].